On the Reliability of Sodium Metal Anodes – The Influence of Neglected Parameters

Author Names: Rico Rupp*, Alexandru Vlad[z]

Affiliation(s): Institute of Condensed Matter and Nanosciences, Molecular Chemistry, Materials and Catalysis, Université catholique de Louvain, Louvain-la-Neuve B-1348, Belgium

[z]alexandru.vlad@uclouvain.be

Abstract

Sodium metal is an auspicious, sustainable alternative to be used in next generation rechargeable batteries. During the past years, a considerable effort was put into finding suitable chemistries, electrode designs, cell setups, and test configurations to enable the safe and efficient use of sodium metal electrodes. With the hunt for ever-increasing coulombic efficiencies and dendrite suppression, the understanding of basic influencing factors is thereby often neglected. Here, we show that not only the basic and so far most studied cell elements, namely electrolyte, separator and substrate, have an impact on the performance of sodium metal anodes. Smallest variations in the amount of electrolyte, current density, cell architecture, and electrode preparation, which are often overlooked, are shown to make the difference between instant cell failure and stable long-term cycling. By optimizing all discussed parameters, we apply the findings and show that stable cycling for more than 1.000 cycles can be achieved with a commercially available electrolyte, if seemingly unimportant factors are considered.

Introduction

Next generation rechargeable batteries that go beyond the currently leading lithium-ion technology and replace lithium with sodium, awakened high interest in the past [1]. This is mainly due to the high natural abundance and low cost of sodium, as well as the possibility to use aluminum as a light and inexpensive current collector. Designing a suitable anode, however, is still a major problem. Avoiding host materials for ions and using sodium metal as an anode would be the ideal case, since metal anodes - Na as well as Li - offer theoretically the highest possible energy density in the respective batteries [1,2]. Failure due to dendrite growth and persistent decomposition and consumption of electrolyte, however, still preclude the application of metal anodes. Finding a solution to these problems is furthermore rendered difficult by the simultaneous influence of many battery elements [3], including - but not limited to - the electrolyte, separator, nature of the current collector, cell architecture, the cycling procedure and cross-talking between the chemical species generated at cathode and anode electrodes. One might find himself for example discarding an electrolyte, because the respective half-cells fail after a few cycles, while a simple change of the utilized separator could have led to hundreds of stable cycles.

Facing the problem of dealing with many interacting components within a commonly used half-cell, a comparative study of several different influence factors is conducted here as a baseline for further improvements of Na-metal anodes. The need for this has previously been expressed[3,4] and most researchers working on the electrochemistry of Na-metal - applied either as working or counter/reference electrodes - will know the struggle of achieving reproducible cycling results. As we will detail next, this apparent irreproducibility is also the result of small variations in the above-mentioned parameters. If one was to neglect them, their effect could be misleading with regard to the actual research topic, and thus result in arriving at an incorrect conclusion.

Since the number of different influence factors is too large for an exhaustive and detailed study within the scope of the here presented work, we focus on several common and less commonly observed factors, as well as a guideline for preparation and assembly of all half-cell components. We also highlight the importance of data analysis, representation and reproducibility, since protocols that might be adequate when Na host materials are used are not necessarily sufficient for Na-metal electrodes. Many shortcomings of a cell can for example be hidden by representing the performance by means of an average of the coulombic efficiency, as is done frequently in literature. A *stability factor* is thus proposed as a simple way of taking dendritic growth into account without the need of using a different cycling protocol.

Experimental

Coin cell assembly

All cells that are discussed in the following were assembled within an argon-filled glovebox in form of half-cells with Na metal counter/reference electrode and a metallic foil as substrate/working electrode. Several commercially available metal foils were used and the influence of material, as well as surface morphology and preparation, was analyzed. A gasket with an internal diameter of 8 mm was cut from 45 µm thick high-density polyethylene (HDPE) foil (Scancell Folien-Vertriebs GmbH) and added on top of the working electrode substrate. HDPE was used, since it is electrochemically stable in all tested electrolytes. Note that Teflon is avoided, since presence of metallic sodium can lead to defluorination of the Teflon surface (turns black) in certain electrolytes. The use of a gasket was found to be essential for reliability and stability as discussed in the results section. To avoid electrical short circuits, a separator was added between the two electrodes and soaked with the respective electrolyte. The required amount of electrolyte was added with a micropipette. Two thirds of the total electrolyte amount were added directly on the substrate, wetting the working electrode, the HDPE gasket and the consecutively added separator. Well-wetting electrolytes can instantly soak the latter one through capillary forces, while unsuitable electrolytes do not penetrate into the separator. One third of the total amount is added on top of the separator to facilitate complete wetting of all other exposed surfaces within the coin cell. In order to study the influence of separator, type of electrolyte, and amount of electrolyte on cell performance, these factors were varied one by one within several sets of experiments (details on the electrolyte composition, exact amount, and separator types are given in the respective sections, including Tables 1 and 2).

A stainless steel (SS-316) disc and spring were added on top of the sodium chip to guarantee even pressure. The cell components are then crimped inside a CR2035 coin cell case (SS-316). An exploded view of the half-cell is shown in Figure 1. As often seen when new electrolytes are tested, symmetric Na-Na cells could be assembled by exchanging the metallic foil with a second Na chip. This can for example be beneficial for the observation of a change in cell overpotential due to electrolyte decomposition and other phenomena. In this work, however, exclusively asymmetric half-cells are discussed, since they give more information about the effect of the substrate and of dead sodium on the cycle-to-cycle stability.

Sodium counter electrode preparation

Sodium (99.9 %) was purchased from Sigma-Aldrich in form of cubes immersed in mineral oil. Na chips were prepared within an argon-filled glovebox. The excess mineral oil was first roughly wiped off, before the cubes were further cleaned in dimethyl carbonate (DMC). The outer layer of the cubes was then cut away with a utility knife in order to remove

oxides and other impurities. The pure sodium was consecutively sandwiched between two layers of HDPE foil and rolled to a thickness of approximately1 mm. Chips with a diameter of 16 mm were finally stamped out of the rolled Na with a circular polypropylene (PP) cutter.

Attention was given to having a smooth Na surface, since it has been shown that a high roughness of the counter electrode can negatively impact the cycling behavior of half-cells [5]. The atmosphere within the glovebox was furthermore controlled carefully. Sodium is not only sensitive to moisture and oxygen content, which are typically monitored and ideally kept below 0.1 ppm, but also to solvents (usually coming from the use of electrolytes) that can be accumulated in the glove-box atmosphere. A solvent sensor and solvent trap (below 2ppm total Volatile Organic Compounds (VOC) content in the glove box for the current work) are thus highly recommended. Alternatively, if a VOC sensor is not available, a good indication for impurities in the atmosphere is that the freshly cut Na chips lose their shine before being assembled. If this is the case, actions have to be taken to avoid contamination.

Substrate preparation

Metallic foils that are used as substrates are often contaminated with organic compounds left over from the manufacturing and handling process, which were removed before introduction into the glovebox. Simple rinsing of the foils with solvents was found not sufficient to remove all organic impurities. For proper degreasing, a Soxhlet extractor with acetone as solvent was used for at least 20 rinsing cycles. The effectiveness of the degreasing process was tested with a simple water break test (water spreads on a clean surface, while it forms droplets with a high contact angle on an insufficiently cleaned film). In addition to degreasing of the substrate, its native oxide layer can be removed. In the case of copper, this can be done by immersing the degreased foils in 5 % sulfuric acid for 15 s. If not mentioned otherwise, however, the foils used here were left with their native oxide.

Other than copper foil substrate (Cu; electrodeposited; 9 µm; 99.8 %; MTI corporation), which is typically used for battery applications, also the effect of aluminum (Al; rolled; 25 µm; 99.5+ %; TOB new energy), nickel (Ni; rolled; 20 µm; 99.9 %; Goodfellow Cambridge), titanium (Ti; rolled; 20 µm; 99.6+ %; Goodfellow Cambridge), and stainless steel (SS; rolled AISI 304; 20 µm; Goodfellow Cambridge) substrates was tested.

Cycling

After cell assembly and a resting period of 12 h to allow complete wetting of the electrodes and the separator, the standard cycling procedure for the half-cells tested in this work consisted at first in a slow galvanostatic step from OCV to 0.01 V (vs. Na^+/Na^0), followed by 10 pre-cycles done at the same low current density of 50 µA/cm^2 between 0.01 and 1 V. This allows to preform part of the solid-electrolyte interface (SEI) on the working electrode. We noticed that in the absence of these pre-cycles, relatively large variations in cycling behavior can appear in the first cycles of the consecutive galvanostatic cycling, since

a missing SEI can influence polarization, nucleation, and the amount of actually plated sodium. It should be noted here that this pre-cycling procedure, while improving the cell stability, does not prevent further SEI formation during the first few cycles completely. This could be due to a difference in SEI formation during the actual Na plating as compared to the pre-cycling, or due to a non-optimized pre-cycling procedure. A charge of 1 mAh/cm^2 for deposition and a stripping cut-off potential of 1 V were chosen as a standard in this work. The half-cell cycling was done on a Neware BTS-(5V-10mA or 5V-50mA) battery tester and the impact of different current densities has been analyzed.

Results and Discussion

Data analysis

The most commonly used parameter to characterize Na or Li half-cells (or in general, the reversibility of the plating-stripping process of a metal) is the coulombic efficiency (CE) defined as the ratio between the charge amount required for the oxidation (C_n^{ox}, also termed as stripping) to the charge amount to reduce (C_n^{red}, also termed as plating) within one full electrochemical cycle (n). The average CE is then typically estimated based on a given number (N) of electrolytic cycles according to Equation 1:

$$CE_N = \frac{1}{N}\sum_{n=1}^{N}\frac{C_n^{ox}}{C_n^{red}} \qquad (1)$$

The electrochemical decomposition of electrolyte during plating, for example, decreases the average CE (with 100 % being the ideal case) and is thus correctly represented by this value. The same is true for incomplete stripping due to the appearance of dead sodium, which are dendrites that are locally thinned down to the point of detaching from the working electrode during stripping. However, certain negative effects can increase the apparent value of CE_N without being beneficial for the system. This includes short circuits due to dendritic growth that are interrupted after a short time period, and anodic side reactions. Fluctuations of the cycle-to-cycle efficiency of a half-cell can furthermore appear due to the reconnection of dead sodium in subsequent cycles. This means that CE_N does not represent these effects correctly and is not sufficient for a complete characterization.

An approach to solve the issue of a misleading average CE value due to the effects described above has first been introduced by Aurbach et al. [6] and has more recently been discussed in detail by Adams et al. [7]. The general idea is to first deposit an excess amount of metal and then to cycle the cell to a limited lower capacity. After a selected number of cycles, a final complete stripping step is used to determine the average coulombic efficiency. This has the advantage that the metal is not completely stripped from the substrate during cycling, neglecting the effect of the substrate and nucleation thereon. Incomplete stripping gives indeed a more accurate representation of the working principle in an actual Na-metal battery. However, only an average CE value can be gained and variations in the cycle-to-cycle

behavior are ignored and averaged in the end. This includes for example the above-mentioned appearance of dead sodium. Complete stripping is furthermore most commonly utilized in literature due to its simplicity as compared to the here explained method. It also allows to single out the effects of different substrates and other influence factors, as well as to conform to the most commonly encountered procedures in literature. The focus of this work was thus set on the standard procedure with complete stripping to 1 V after each deposition cycle. The mentioned method with incomplete stripping, however, was used in addition for selected parameters and is discussed later on.

Furthermore, to quantify the cycle-to-cycle stability of the CE in the case of complete stripping, which is reduced by the appearance of reversible dead sodium, a stability factor S is introduced here. The higher S is, the less variation there is in the coulombic efficiency CE_n over N cycles:

$$S = \frac{N}{\sum_{n=1}^{N} |CE_n - 2CE_{n+1} + CE_{n+2}|^2} \qquad (2)$$

It is worth mentioning that plotting the coulombic inefficiency (CI; see Equation 3) can be beneficial in certain cases, for example when comparing several cell results. In contrast to the coulombic efficiency, the CI (Equation 3) can often give a more detailed view on small variations close to 100 % CE (or equivalent to 0 % CI), since it allows visualization on a logarithmic scale. Plotting the CE on a linear scale from 0 to 100 % can easily hide certain shortcomings of the respective cell.

$$CI_n = 1 - CE_n = 1 - \frac{C_n^{ox}}{C_n^{red}} \qquad (3)$$

However, due to local fluctuations to values above 100 % CE caused by the reconnection of dead sodium and short-lived short circuits, the CI is only used for average cell values and not to show the evolution of one cell with cycling, since it would result in negative values.

Electrolytes – carbonates vs. glymes

Electrolytes are one of the most commonly observed variables for Na and other metal batteries, being an integral part of any cell. Several common liquid electrolytes are discussed hereafter. Apart from having a sufficiently high ionic conductivity, a suitable liquid electrolyte should wet the separator and electrodes, it should form a stable SEI from the early stages on to prevent further electrolyte decomposition, and promote non-dendritic sodium plating. Electrochemical stability at high potentials is furthermore required if a high voltage Na-metal battery is to be made operational. With all these requirements and the importance of fulfilling every one of them, it is no wonder that the number of different electrolyte compositions that can be found in literature, or that are commercially available, is continuously increasing [3]. Not only solvents and salts are thereby varied, but also additives and salt concentration are subjects of interest. Considering this, an exhaustive list of electrolytes cannot be given here. However, a range of common, commercially available

liquid electrolytes has been tested in combination with different separators and substrates.

The herein used electrolyte salts are sodium perchlorate ($NaClO_4$), sodium hexafluorophosphate ($NaPF_6$), sodium bis(fluorosulfonyl)imide ($NaN(SO_2F)_2$ - NaFSI), and sodium trifluoromethanesulfonate ($NaCF_3SO_3$). The electrolyte solvents used are ethylene carbonate (EC), diethyl carbonate (DEC), dimethyl carbonate (DMC), propylene carbonate (PC), diethylene glycol dimethyl ether (G2), tetraethylene glycol dimethyl ether (G4), or combinations thereof. All electrolytes were tested at < 1 ppm water content. Fluoroethylene carbonate (FEC) was used as an additive for two of the electrolytes. All electrolytes were used in conjunction with glass microfiber filters (GF/D) and Celgard separators (CG), which are further detailed in a dedicated section (where also other separators are used together with the most promising electrolyte). This is also the case for the substrates. The tested combinations are listed in Table 1 and the respective average CI over 40 cycles and smoothness parameters are mapped in Figure 2. General trends are indicated for groups of electrolytes that show comparable results, independently of the substrate and separator, which are discussed later. It should be noted that these trends could vary if any of the other parameters is altered, as discussed next.

In general, as already reported, carbonate-based electrolytes were observed to be the least suitable. Under the here applied conditions, they all suffer from dendritic or mossy growth, formation of dead sodium, and continuous electrolyte decomposition. This leads to the formation of a thick, electrically insulating layer of dead Na and SEI. Since this layer hinders Na^+ diffusion towards the substrate, an increasing polarization can be observed with ongoing cycling, as is shown exemplary in Figure 3a. A SEM micrograph is shown in Figure 3d after 10 cycles with $NaClO_4$:EC/DEC electrolyte, showing the inhomogeneous, dendritic morphology that is typical for the discussed carbonate-based electrolytes.

A FEC additive (5 vol.-%) can improve the performance of the respective electrolytes to about 20 % CI by stabilizing the SEI and by slightly refining the morphology (Figure 3e). However, the same problems persist, as can be seen in Figure 3b and c. A thick layer consisting of dead Na and SEI is built up during cycling. Dugas et al. studied the continuous decomposition on $NaPF_6$:EC/DMC and found that FEC can alter the reaction products of the electrolyte decomposition, but not stop it [8]. Note that the kink in the plating potential (Figure 3, with and without FEC) is due to dendritic growth and the formation of dead Na at the counter electrode. Wood et al. explained this for Li-metal anodes by using in situ optical microscopy [9]: It is easier to strip dendrites, rather than bulk Na. Since plating on the working electrode implies stripping from the counter electrode, the necessary overpotential increases when no more dendrites are electrically connected to the counter electrode and pitting occurs (Figure 3b). The coulombic efficiency initially improves with cycling (increased capacity on charge), since the SEI formation slows down, but does not stop completely. Since more Na is plated on the counter electrode (during charge), more dendritic Na is available on the counter electrode to be stripped during the consecutive discharge, resulting in a delayed appearance

of the kink (indicating the change from stripping of dendritic Na to stripping of Na bulk). A slight change of morphology due to the build-up of dead Na and SEI could possibly also contribute to the increase of dendrites on the counter electrode.

Among all tested electrolytes only $NaCF_3SO_3$ in diglyme or tetraglyme allowed stable cycling with a low CI. Seh et al. attribute the better cycling behavior of ether-based electrolytes, as compared to carbonate-based electrolytes, to a more uniform and compact SEI, comprising mainly inorganic components (Na_2O and NaF) [10]. They state that also the choice of the salt contributes to a favorable SEI chemistry, explaining why $NaClO_4$:G2 has such a high CI (Figure 2). The SEI chemistry, however, cannot always be fully accounted for cell failure. Many other parameters, some on which will be elaborated hereafter, can for example influence the morphology of deposited Na and impact the formation of dead Na, the amount as well as the dissolution of formed SEI (independent of its chemistry), and more. The microporous, mossy morphology that is observed when $NaCF_3SO_3$:G2 is used as an electrolyte, as compared to the dendritic morphology of the carbonate-based electrolytes under the same conditions, is shown in Figure 3f. $NaCF_3SO_3$:G2 will be used to show that stable cycling for more than 1000 cycles can be achieved if seemingly unimportant factors are considered and adapted.

Separators

Separators have to fulfill several main requirements in order to be usable in the respective cell. They have to be electrically insulating, chemically stable, and porous, what allows for soaking with an ionically conductive liquid electrolyte. Another requirement for the separator is thus to be well permeable and wettable by the electrolyte. Pore size, pore distribution, tortuosity, and thickness of the separator can furthermore influence the morphology and thus the performance of the cell, since they alter the distribution of current density and Na^+ concentration. These properties have already been subject of intensive studies [11,12]. Other attributes that impact mainly safety aspects are mechanical strength, dimensional stability, thermal shrinkage, and the ability of thermal shutdown [13].

With all the above-mentioned parameters, it is not astonishing that the proper choice of separator is essential for a well performing cell. The results in Figure 2 include half-cells assembled with different kinds of separators combined with the respective electrolyte (refer to Table 2 for details). GF/D (120 µl electrolyte) and CG (40 µl electrolyte) were tested for all electrolytes, while the others were only tested for the most promising one ($NaCF_3SO_3$:G2). Depending on the electrolyte, the effect of a certain separator on the cell performance can vary drastically. General trends can thereby be observed:

- Carbonate-based electrolytes perform better with a GF/D than with CG separator. This is most likely due to the larger amount of electrolyte that is absorbed by the GF/D. Since

these cells suffer from severe electrolyte decomposition, large electrolyte excess can retard the inevitable cell failure.

- PC- and DMC-based electrolytes have a large contact angle on PP and do not wet CG separators well. This leads to instantaneous cell failure due to overpolarization, since the electrolyte does not penetrate the separator completely.

- When using $NaCF_3SO_3$ in G2 or G4, all separators except CG lead to a short circuit within the first 1-12 cycles. An example is shown in Figure 4 for a GF/D separator cycled with $NaCF_3SO_3$:G2 on copper as working substrate electrode. Mossy or dendritic Na grew between the fibers of the separator and detached from the copper substrate during disassembly of the coin cell. The other side of the separator showed that the separator was penetrated completely in one of the spots, leading to failure of the cell. The better performance of CG for these electrolytes could be due to a more homogeneous current density, a more favorable distribution of the Na^+ concentration, or physical hindrance of dendritic growth through the nanoscale pores of the CG separator.

Current density

In literature, cycling efficiency and stability is often considered to improve with decreasing current density, since dendritic growth is less likely [14]. However, as can be seen in Figure 5, an optimal current density - here around 2 mA/cm^2 - was found for $NaCF_3SO_3$:G2 electrolyte on copper substrate. Higher values lead as expected to more dendritic, less dense, and therefore less stable deposits. However, also low values can influence the cells negatively. Similar to observations that have been made for lithium, needle-like dendrites are expected at low current densities, as opposed to fractal dendrites at high current densities and mossy/porous sodium at intermediate values [15]. Fractal dendrites grow only at their tip once the respective Sand's time is reached, whereas needle-like dendrites can also grow at kinks and roots. Either of these two cases can lead to short circuits. Since nucleation and growth of dendrites is to some extent a statistical process and smallest fluctuations of the plating conditions can influence them, it is difficult to give a concrete value of a current density for which short circuits will appear. While no short circuits were observed at 2 mA/cm^2, even up to 1200 cycles, the probability for cell failure increases rapidly when veering away from this optimum.

A high current density can furthermore affect not only the plating behavior, but also stripping of sodium. As previously observed for lithium, a higher stripping current density can increase the CE [16]. This can most likely be ascribed to a lower amount of dead Na when excessive stripping at the base of deposits is avoided. Independent variation of plating and stripping current density was however not performed in our work. Another influence factor of current density is the lower nucleation density and therefore growth of a less uniform and less

dense deposit at low values [17]. The dependence of nucleation density was previously observed for lithium and is supported by classical nucleation theory [18,19]. A more uniform deposit minimizes the surface area of the electrode and therefore the amount of SEI that is formed [16]. Even the composition of SEI can be influenced, which will however depend on the utilized electrolyte. A simple variation of current density results in an interaction of all these effects. It finally leads to a non-linear evolution of the half-cell performance as seen in Figure 5, which will depend strongly on the used electrolyte.

It is important to note that the here recorded plating behavior is only valid for the described setup, including all mentioned parameters. A change in plating capacity would for example result in the appearance of fractal dendrites already at lower current densities, as was discussed by Bai *et al.* This complex interdependence of different influence factors is one of the main difficulties in testing Na-metal anodes.

Cell architecture - gasket

Due to their assembly procedure, half-cells are frequently found to contain substrates that are larger than the sodium counter electrode, with the Na chip not filling the entire coin cell. Proper practice in electrochemistry, however, is the use of a counter electrode that is the same size or preferably larger than the working electrode. Even if polarization of the sodium chip might not be the problem here, the distribution of current density at the substrate surface can be influenced by the cell architecture. In order to guarantee the identical (active) area of both electrodes with perfect alignment, the Na chip would need to fill the complete coin cell up to its sealing. Since it is difficult to achieve homogeneous pressure distribution in this case, another option is proposed here: a HDPE gasket is added directly on the substrate (see Figure 1), confining the area in which plating and stripping occurs. In Figure 6, half-cells with and without a HDPE gasket are compared. It can be seen that the average CE within 250 cycles is with 99.6 % slightly higher when a gasket is used, as compared to 99.4 % without a gasket. More importantly, the cycle-to-cycle fluctuation of the CE is altered drastically. While the CE with gasket is certainly not perfect due to limitations of the electrolyte and other factors that are discussed in this article, it fluctuates only a few percent around its average (S = 0.09). The half-cell without gasket, however, is much less stable (S = 0.001). One possible explanation with the 'classical' cell architecture without gasket is that the electric field between the substrate and a small Na chip (smaller than the inside diameter of the coin cell) expands beyond the Na chip coverage area (see Figure 6c). This can result in a difference between nominal and actual plating area, therefore changing the actual average current density. If the Na chip has for example a diameter of 16 mm, but material is plated on the whole accessible substrate with a diameter of 18 mm, a nominal current density of 2 mA/cm^2 would lead to a real average value of 1.58 mA/cm^2. The current density close to the borders of the sodium chip is furthermore expected to be inhomogeneous, as shown in Figure 6c. As was discussed before, the cell performance in this specific case is very susceptible to a

change of current density (see Figure 5), as it influences nucleation density and morphology. Even if only the border of the deposit is altered, the overall impact is still relatively large in a coin cell. The SEM micrograph in Figure 6b shows that the gasket effectively limits the amount of deposited Na that is affected by a change in the electric field to a width of less than 100 µm along the deposit border. This results in a clear separation between Na-deposit and pristine Cu foil. Without a gasket (Figure 6c), on the other hand, the deposit extends several hundred µm (further than can be displayed in the SEM micrograph) beyond the edge of the counter electrode and a more dendritic (worm-like; labeled as Na_{dend}) morphology, as well as Na-islands and a wavy edge can be observed in this extended region.

Electrolyte amount

Similar to the effect of the current density, also the electrolyte amount shows an optimal value, as shown in Figure 7. Several regions can be found in the general trend (red curve). At low volumes (I) the electrolyte does not entirely fill all the pores of the separator. While a 19 mm diameter CG 2325 separator with a porosity of 39 % [11] has a free pore volume of only 2.8 µl (≈ 1 µl/cm^2), about 30 µl (≈ 10 µl/cm^2) are necessary before the cell performance reaches its optimum (II). This is because not only the CG pores are filled, but also all surfaces within the coin cell are wetted with a layer of electrolyte, and its decomposition at low potentials reduces the amount of available liquid even further. If an excess amount of electrolyte is added (III), the performance of the cell decreases again. Based on our analysis, we cannot provide a clear explanation for this observation as further in-depth analysis and experiments might be required. A possible explanation could be that a large amount of electrolyte may negatively influence the performance, if the SEI contains soluble compounds, as was observed for calendar aging of Li-metal cells [20]. Impurities that are contained in the electrolyte, for example traces of water (yet, as measured in our work, all electrolytes have a water content of < 1ppm), can furthermore play an enhanced role in cell deterioration if more electrolyte and therefore a larger amount of impurities is present. Eventually, the amount of electrolyte within the cell saturates (IV), even if the added volume is increased - excess is being pressed out of the coin cell during crimping.

A balance has to be found between incomplete wetting of the Celgard separator at low volumes, and an electrolyte surplus that facilitates SEI dissolution, dendritic growth and therefore the creation of dead sodium. In our case, the ideal volume amounts to about 30 µl (≈ 10 µl/cm^2). This value, however, can vary depending on cell architecture (herein, CR2032 format being used), separator, electrolyte, and pressure used for crimping.

Substrates

In the context of Li or Na metal plating, metallic substrates can generally be divided into *alloying* and *non-alloying*. Alloying is referred here to the respective metal, forming intermetallic compounds with Na at room temperature, with gold being an example in this

category [21]. Non-alloying metals, on the other hand, do not form intermetallic compounds at room temperature. The non-alloying type was chosen here due to this inertness against Na, even if this does not necessarily exclude a certain solubility for sodium in the substrate. While the available phase diagrams of the here chosen metals (Cu[22], Ni[23], Al[24], Ti[25]) do not show a visible solid solubility of sodium at room temperature, their accuracy might be questioned, since they are often based on theoretical models. Even a small amount of dissolved Na could still influence the plating behavior due to a reduced nucleation overpotential [26]. The interaction of Na with stainless-steel (SS) cannot be deduced from a simple phase diagram, since SS contains more complex phases, but it is still safe to assume that it is inert versus Na. Figure 8 shows plating profiles for the chosen substrates. They all exhibit similar behavior regarding the initially high overpotential, which is typical for non-alloying metals, as was discussed by Yan et al. [26].

Figure 9 shows the CE for the first 300 cycles with different substrates. Exemplary cycling profiles are shown for Ti and SS in Figure 10. Both foils are rolled and have a comparable surface roughness. In contrast to the other substrates, titanium led to unstable cell polarization during stripping and increasing plating overpotential with cycling (see Figure 10a). This can be related to an increased amount of reversibly generated dead Na when using a Ti substrate, which is also reflected by its unstable CE. Even though its average CE is as high as 99.68 % over 300 cycles, the cycle-to-cycle stability is relatively low (S = 0.01). Etched copper, on the other hand, led to the highest smoothness parameter (S = 0.07) with an average CE of 99.74 %.

While the effect of the substrate is indisputable, its origin is not as clear. Several possible influence factors should be kept in mind when choosing a substrate. The native oxide layer on metal surfaces can affect sodium plating. In the case of titanium, for example, its dense native oxide layer is likely to cause the initially observed chaotic cycling profiles by altering the sodium morphology and leading to more dead sodium. Even if titanium itself does not form intermetallic compounds, the oxide layer can be sodiated at low potentials and form $Na_xTi_yO_z$ [27]. This can in turn influence the potential profiles, nucleation behavior and efficiency of the electrode. The effect of the native oxide varies however from metal to metal. For Cu, removal of the native oxide led for example to a less predictable stability. Average CE over 400 cycles was decreased from 99.63 ± 0.35 % to 98.56 ± 1.43 % when the oxide was removed prior to half-cell assembly (average of 8 cells; 2 mA/cm^2). A possible cause is an improved nucleation of sodium on copper oxide rather than on pure copper. Similar behavior has been exploited in the past by adding an artificial nucleation layer on an aluminum current collector [28].

It is furthermore expected that not only the choice of substrate metal, but also its surface morphology dictate the plating behavior. The use of structured substrates (porous, nanowires, channels) is a relatively recent trend to improve the cycling stability of Na-metal anodes by avoiding dendritic growth [29–32]. Similarly, but to a lower extend, the surface roughness of

metal substrates could affect cell performance. Electrodeposited Cu foil, for example, has a rough and a smooth side due to its manufacturing process, while rolled foils typically show rolling grooves. This can result in a slight variation of the local current density and affect the nucleation density. In the present work, however, the variation of roughness between foils was too small to draw a reliable conclusion and a systematic study would be necessary to gain deeper insight into the effect of surface morphology on the plating behavior.

Controlling all discussed parameters

The influence of several important parameters on the cycling of Na-metal half-cells - some more and some less obvious - was discussed above. Keeping all these parameters in mind, the benefit of controlling them is displayed hereafter. Since $NaCF_3SO_3$ in glymes showed the best results of all tested electrolytes and the cycling profiles with G2 are more stable than with G4, 1M $NaCF_3SO_3$:G2 was chosen as an electrolyte for the exemplary cell. Copper foil (rough side without removal of its native oxide) was used as substrate, since it yielded the highest stability factor over the whole cycling range. This choice was also further motivated by the industrial applicability of copper, which is not reasonable for the discussed SS, Ni, or Ti foils. Although Al is typically claimed to be a good candidate to replace Cu for next-generation Na-ion cells, it may not be a good replacement for Na-metal cells, judged by the initially low cycling stability (see Figure 9), which might be attributed to the effect of its native oxide layer on Na plating. As shown before, short circuits were only effectively limited by using a CG separator. The amount of electrolyte per cell (CR2032 coin format) was fixed to 30 µl, which was found to guarantee optimal wetting of all cell components. A HDPE gasket was furthermore used to guarantee a homogeneous current density and a well-defined plating area. The cells were precycled between 0.01-1 V at 50 $\mu A/cm^2$ and cycled to 1 mAh/cm^2 at a current density of 2 mA/cm^2 (stripping to 1 V), which was shown to be the optimal value for this setup.

Cycling profiles and the coulombic efficiency until failure are shown in Figure 11a-b. The plateau value of plating overpotential was initially about 35 µV (see Figure 11a) and increased after 1000 cycles to 60 µV. This increase is due to a slight accumulation of (irreversible) dead sodium and SEI at the surface of both electrodes. In addition, local fluctuations of polarization, as seen in Figure 11b (bottom), occurred due to reversible formation of dead Na on the copper substrate as well as on the Na counter/reference electrode. The average CE over 1200 cycles (before degradation and failure of the cell) is 99.74 % (S = 0.030). The increase in CE over the first cycles can be attributed to a relatively slow stabilization of the conditions at the substrate surface. Adams et al. stated that the actual average CE is represented more accurately if this initial stabilization region is ignored [7]. Doing this, the average CE between cycle 50 and 1200 is 99.81 % (S = 0.029), which indicates that the SEI needs several cycles to be completely formed, even with the 10 precycles that were done prior to cycling. A slow decrease of CE after 600 cycles is

furthermore visible and was most likely caused by accumulation of (irreversible) dead Na and SEI. The slightly decreasing stability factor shows furthermore that the amount of dead sodium increases with cycles. For the stable region between 50 and 600 cycles, an average CE of 99.96 % (S = 0.072) was reached.

Even though high average coulombic efficiencies were reached, one of the most severe problems in cycling of these cells can be seen at the end of the cell lifetime (Figure 11b; > 1200 cycles): the CE starts decreasing, indicating the accumulation of dead sodium, which in turn hinders Na^+ flux and increases local current densities. This leads to a less homogeneous plating process and can eventually alter the morphology of deposited Na, if the (reversible) dead sodium is not stripped in time. When shifted towards more dendritic growth, the amount of dead Na is increased further - a self-accelerating process that eventually leads to failure of the cell due to short-circuiting. Apart from being a safety issue in real applications, this is also a problem, since failure in this system is not a steady process, but rather a sudden and non-predictable event. Figure 11c shows the good reproducibility of the general cycling behavior when the cells are assembled under well-controlled conditions. While their failure can be delayed by improving these conditions, the actual lifetime cannot be predicted accurately and is to a certain extend a statistical phenomenon. If impurities are however introduced through the atmosphere of the glove box during cell assembly, as shown in Figure 11d, rapid failure occurs even without the above-described self-accelerated accumulation of dead Na.

As was discussed before, a more realistic and accurate average CE can be achieved by incomplete stripping of excess sodium [7]. Half-cells were thus assembled and cycled with the same parameters as mentioned above, with the difference that an initial capacity of 4 mAh/cm² was plated on the substrate before cycling at a limited capacity of 1 mAh/cm². This resulted in an improved average CE of 99.89 ± 0.02 % for 200 cycles when sodium is not stripped completely, as compared to 99.52 % for the first 200 cycles with complete stripping to 1 V. The better results of incomplete stripping for short cycling times could suggest that in our case dead sodium detaches mainly at late stages of the stripping process when the mossy Na structures are locally thinned down enough to lose contact to the substrate. Another possibility is that the SEI is less stable when the electrode is cycled up to higher potentials, which would not be the case in an actual battery. For longer cycling, this method leads to sudden polarization at the end of the stripping steps when the Na reservoir is exhausted. Under the described conditions, this was found to be the case at cycle 652 ± 123, resulting in an average CE of 99.53 ± 0.10 % (average for 4 cells), and confirming that the amount of dead sodium increases with prolonged cycling.

While a higher stability parameter would still be aspired and self-accelerated accumulation of dead Na remains to be solved, these values are far beyond the previously reported performance of this electrolyte under similar conditions[10].

This illustrates that new electrolytes and other cell components should not directly be

discarded because they show poor performance under certain conditions. The complex interaction between many factors has to be taken into account when working with Na-metal anodes, and the importance of often-neglected parameters on the cycling performance should be borne in mind. While the above-described processes and conditions for the preparation of electrodes, the coin cell assembly and cycling, apply broadly and general trends are pointed out, many of the determined optimal parameters are not universally applicable. A change of the electrolyte can for example influence the optimal values for many of the discussed parameters. When introducing variations to the system that was employed above as an example, it is thus recommended to use the respective values only as a starting point for the case-specific determination of appropriate parameters.

Conclusions

A selection of frequently discussed, as well as often-neglected parameters has been tested on their importance for cycling of Na-metal half-cells. It was found that every single one of the tested parameters influences cell performance to a variable extent. The tested variables include electrolyte, separator, nature of the current collector, electrode preparation, cell architecture, and the cycling procedure. In many cases, their effects are interconnected, resulting in a complex system, which is very susceptible to changes. Detailed attention is to be payed to seemingly trivial aspects of cell assembly and cycling in order to achieve reproducible results. It was furthermore shown that control of these influence factors is necessary to achieve stable and reproducible cycling. More than 1200 cycles at an average coulombic efficiency of 99.74 % (S = 0.030), with up to 99.96 % (S = 0.072) over a range of 550 cycles, was achieved for a commercial electrolyte ($NaCF_3SO_3$:G2). To the best of our knowledge, this electrolyte has not yet been reported to allow for a comparable performance in half-cells. It has to be clarified, however, that the susceptibility of the tested system to small changes in the experimental parameters is a severe problem that might render it unusable in reality, even though a high CE can be reached. This emphasizes the influence of neglected parameters and the importance to consider these when testing new materials or when trying to reproduce results.

Acknowledgments

Rico Rupp is a Research Fellow at the Belgian *Fonds de la Recherche Scientific* (F.R.S-FNRS). This work was also supported by FNRS - U.N011.18 - DEMIST and CF-ARC (18/23-093) MICROBAT research grants.

References

1. X. Zheng et al., *Energy Storage Mater.*, **16**, 6–23 (2019).
2. X.-B. Cheng, R. Zhang, C.-Z. Zhao, and Q. Zhang, *Chem. Rev.*, **117**, 10403–10473 (2017).
3. Y. Zhao, K. R. Adair, and X. Sun, *Energy Environ. Sci.*, **11**, 2673–2695 (2018).
4. D. S. Tchitchekova et al., *J. Electrochem. Soc.*, **164**, A1384–A1392 (2017).
5. J. Conder and C. Villevieille, *Chem. Commun.*, **55**, 1275–1278 (2019).
6. D. Aurbach, O. Youngman, Y. Gofer, and A. Meitav, *Electrochim. Acta*, **35**, 625–638 (1990).
7. B. D. Adams, J. Zheng, X. Ren, W. Xu, and J. G. Zhang, *Adv. Energy Mater.*, **1702097**, 1–11 (2018).
8. R. Dugas et al., *J. Electrochem. Soc.*, **163**, A2333–A2339 (2016).
9. K. N. Wood et al., *ACS Cent. Sci.*, **2**, 790–801 (2016).
10. Z. W. Seh, J. Sun, Y. Sun, and Y. Cui, *ACS Cent. Sci.*, **1**, 449–455 (2015).
11. M. F. Lagadec, R. Zahn, and V. Wood, *Nat. Energy*, **4**, 16–25 (2019).
12. N. Li et al., *Nano Lett.*, **18**, 2067–2073 (2018).
13. S. S. Zhang, *J. Power Sources*, **164**, 351–364 (2007).
14. P. Bai, J. Li, F. R. Brushett, and M. Z. Bazant, *Energy Environ. Sci.*, **9**, 3221–3229 (2016).
15. K. N. Wood, M. Noked, and N. P. Dasgupta, *ACS Energy Lett.*, **2**, 664–672 (2017).
16. J. Qian et al., *Adv. Funct. Mater.*, **26**, 7094–7102 (2016).
17. S. Lv et al., *Nat. Commun.*, **9**, 2152–2163 (2018).
18. A. Pei, G. Zheng, F. Shi, Y. Li, and Y. Cui, *Nano Lett.*, **17**, 1132–1139 (2017).
19. J. Mostany, B. R. Scharifker, K. Saavedra, and C. Borrás, *Russ. J. Electrochem.*, **44**, 652–658 (2008).
20. S. M. Wood et al., *Adv. Energy Mater.*, **1801427**, 1–6 (2018).
21. A. D. Pelton, *Bull. Alloy Phase Diagrams*, **7**, 136–139 (1986).
22. H. Okamoto, *J. Phase Equilibria Diffus.*, **37**, 350–362 (2016).
23. B. Predel, in *Li-Mg – Nd-Zr. Landolt-Börnstein - Group IV Physical Chemistry (Numerical Data and Functional Relationships in Science and Technology)*, O. Madelung, Editor, vol. 5H, p. 1, Springer, Berlin, Heidelberg (1990).
24. S. Zhang, Q. Han, and Z. K. Liu, *J. Alloys Compd.*, **419**, 91–97 (2006).
25. C. W. Bale, *Bull. Alloy Phase Diagrams*, **10**, 138–139 (1989).
26. K. Yan et al., *Nat. Energy*, **1**, 16010 (2016).
27. J. Libich et al., *ECS Trans.*, **74**, 313–319 (2016).
28. A. P. Cohn, N. Muralidharan, R. Carter, K. Share, and C. L. Pint, *Nano Lett.*, **17**, 1296–1301 (2017).
29. C. Wang, H. Wang, E. Matios, X. Hu, and W. Li, *Adv. Energy Mater.*, **1802282**, 1–11 (2018).
30. X. Wang et al., *Nat. Energy*, **3**, 227–235 (2018).
31. Y. Xu et al., *Energy Storage Mater.*, **12**, 69–78 (2018).
32. W. Luo et al., *Nano Lett.*, **17**, 3792–3797 (2017).

Tables:

Table 1: Combinations of electrolytes, substrates, and separators that were used for half-cell assembly and testing in Figure 2. Details about the substrates and separators are given in the respective dedicated sections.

Salt	Solvent(s)	Substrates	Separators
$NaClO_4$	EC/DEC (1:1)	Cu; Al	Celgard; glass fiber
$NaPF_6$	EC/DEC (1:1)	Cu; Al	Celgard; glass fiber
NaFSI	EC/DMC (1:1)	Cu; Al	Celgard; glass fiber
$NaClO_4$	PC	Cu; Al	Celgard; glass fiber
$NaClO_4$	EC/DEC (1:1) + 5 % FEC	Cu; Al; Ni; SS	Celgard; glass fiber
$NaClO_4$	G2	Cu; Al; Ni; SS	Celgard; glass fiber
$NaCF_3SO_3$	G2	Cu; Al; Ni; SS	Celgard; glass fiber
$NaCF_3SO_3$	G4	Cu; Al; Ni; SS	Celgard; glass fiber
$NaCF_3SO_3$	G2 + 5 % FEC	Cu; Al	Celgard; glass fiber

Table 2: Separators for half-cell assembly.

Filter	Material	Pore size
Whatman glass microfiber filter (GF/D)	borosilicate	2.7 µm
Celgard 2325 (CG)	PP/PE/PP	0.21x0.05 µm
Whatman track etched membrane (PC8)	PC	8 µm
Whatman track etched membrane (PC0.4)	PC	0.4 µm
Millipore woven net filter (nylon)	Nylon	0.45 µm
Grade 413 filter paper (FP)	cellulose	5-13 µm

Figures:

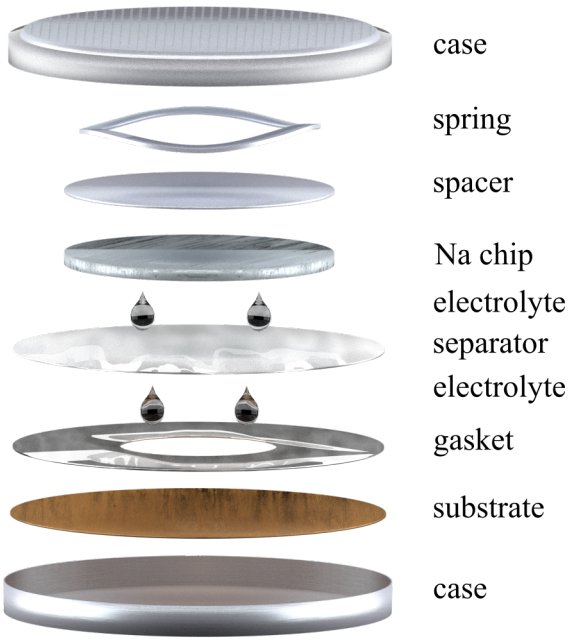

Figure 1: Elements of the proposed coin cell (CR 2032 format, SS-316 material) architecture with HDPE gasket.

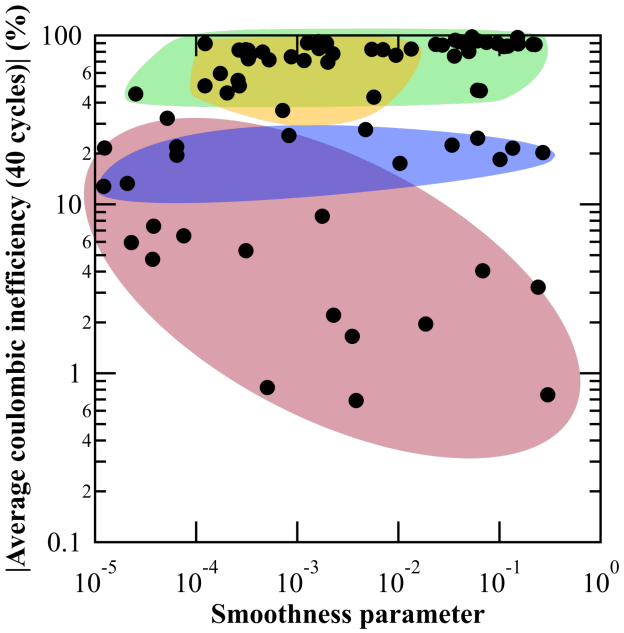

Figure 2: Average CI (over 40 cycles) plotted versus smoothness parameter (S) for half-cells cycled at 0.5 mA/cm^2, 1 mAh/cm^2 and an upper stripping potential of 1 V. Variations of half-cells were assembled with a celgard separator (40 µl electrolyte) or with a glass fiber separator (120 µl electrolyte), as well as with copper, aluminum, nickel, and stainless steel substrates. General trends are marked irrespective of the separators and substrates for several carbonates (green), carbonates with FEC additive (blue), $NaClO_4$ in G2 (yellow), and $NaCF_3SO_3$ in G2 or G4 (red).

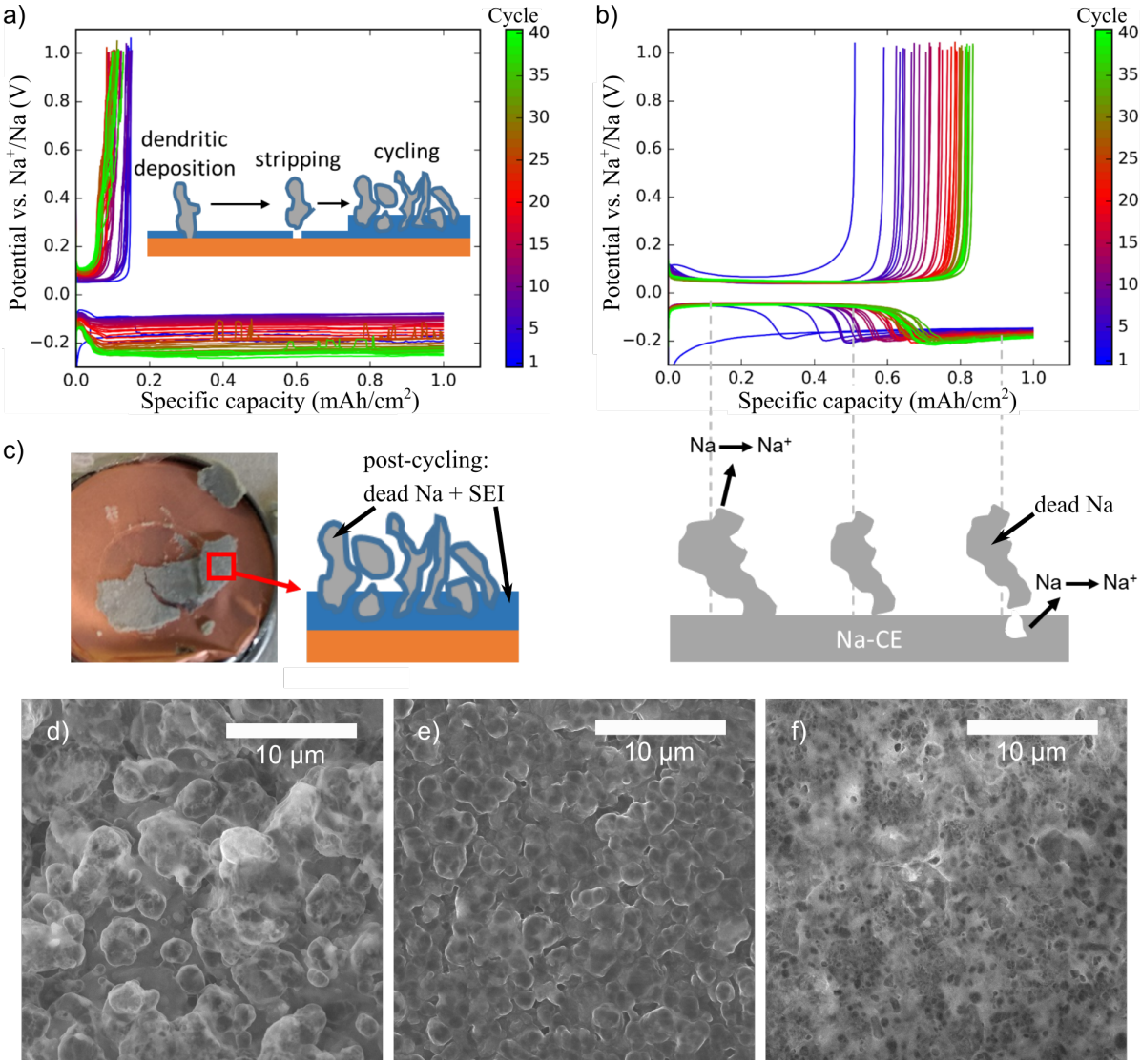

Figure 3: a) Cycling profiles for a cell with the following characteristics - 120 µl $NaClO_4$:EC/DEC electrolyte in GF separator and cycled at 0.5 mA/cm^2, HDPE gasket, Cu foil working substrate. b) Cycling profiles after addition of 5 % FEC to the electrolyte and the origin of kinks in the potential profile during plating due to dendrite formation on the Na metal counter electrode. c) Post-cycling image of the FEC-containing cell with a residual layer of dead sodium mixed in SEI on the copper substrate. SEM micrographs of Na-deposits after 10 cycles for d) $NaClO_4$:EC/DEC, e) $NaClO_4$:EC/DEC/5% FEC and f) $NaCF_3SO_3$:G2 cells.

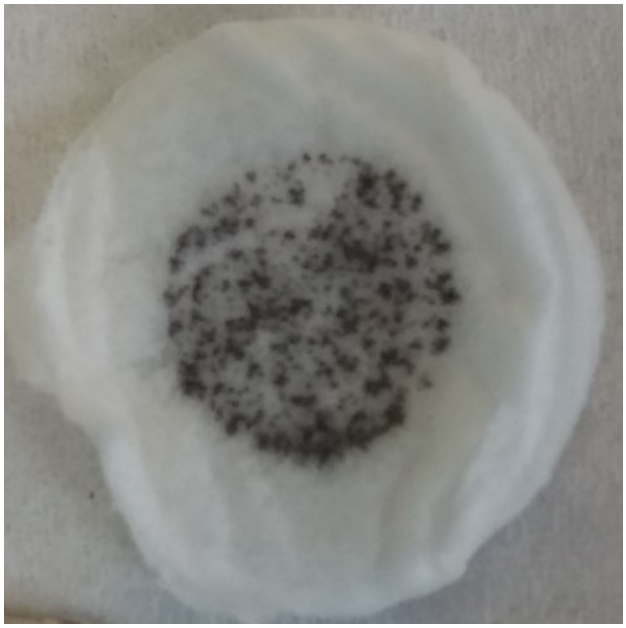

Figure 4: GF/D separator after the half-cell with $NaCF_3SO_3$:G2 failed (7th cycle). The visible side was facing the copper foil. The dark spots are dendritic Na structures that grew into the pores of the separator and detached from the substrate during cell disassembly. One dendrite was visible on the backside of the separator and caused a short circuit.

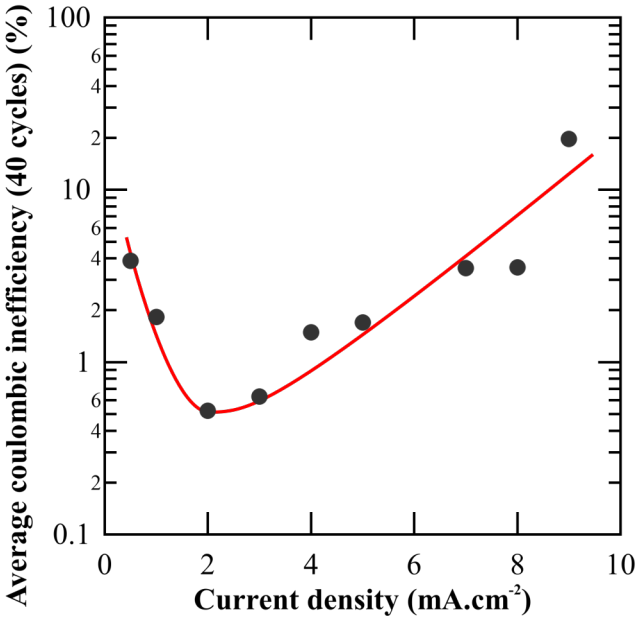

Figure 5: Influence of the current density on the average CI over 40 cycles when cycled with 30 µl of $NaCF_3SO_3$:G2 electrolyte, CG separator, on Cu substrate, and a capacity of 1 mAh/cm^2. Note that 0.25, 6, 10, and 20 mA/cm^2 resulted in (reversible) short circuits within the first 40 cycles, therefore distorting the actual CI. The results from these values are thus not shown here.

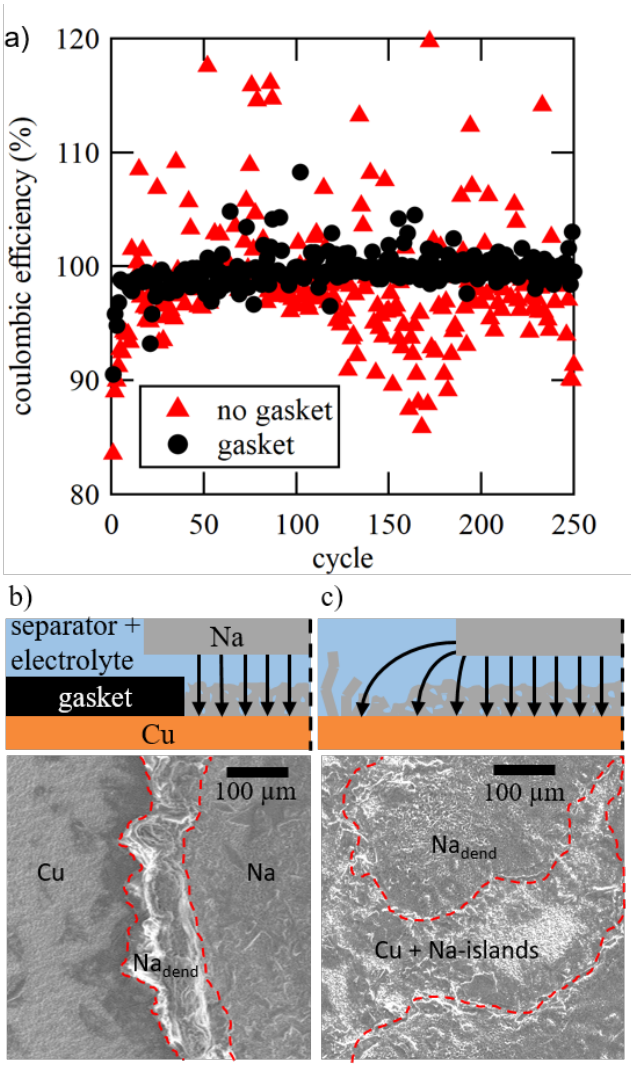

Figure 6: a) Impact of a HDPE gasket on the CE of a half-cell. Cycled with 30 µl of $NaCF_3SO_3$:G2 electrolyte and CG separator on Cu substrate at 2 mA/cm^2 (nominal current density with respect to the area confined by the gasket). b) and c) Schematic of the expected current density distribution (black arrows) for half-cells with and without HDPE gasket respectively and corresponding SEM micrographs at the border of the deposit (indicated by the dashed red line) after 10 cycles.

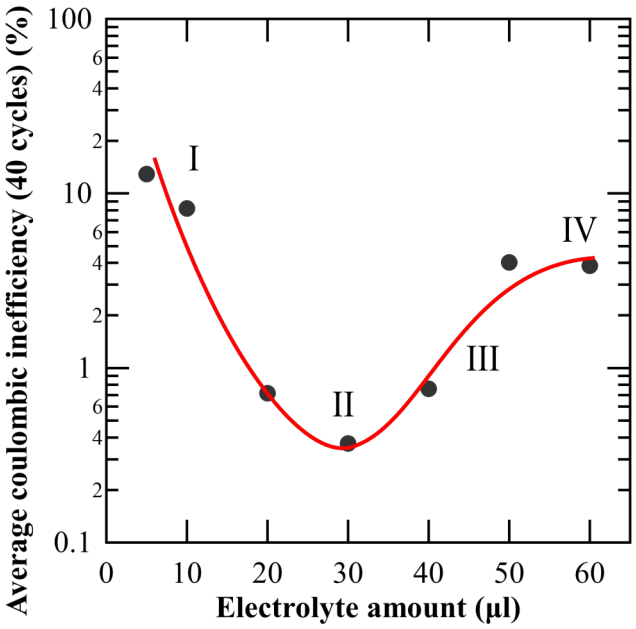

Figure 7: Influence of the amount of electrolyte on coulombic inefficiency for $NaCF_3SO_3$:G2 electrolyte with a CG separator, HDPE gasket, Cu substrate, and operated at 2 mA/cm^2.

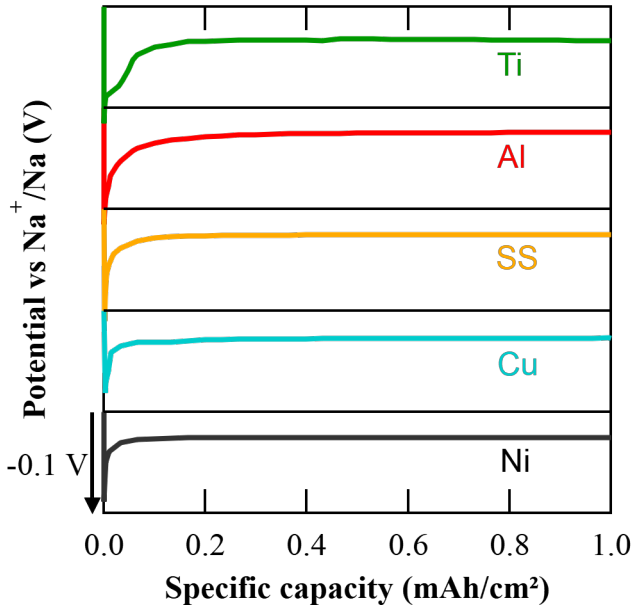

Figure 8: Plating profile of the third cycle for all tested substrates. The half-cells were cycled at 2 mA/cm² with 30 µl $NaCF_3SO_3$:G2 and CG separator. The initially high overpotential indicates nucleation on a non-alloying substrate.

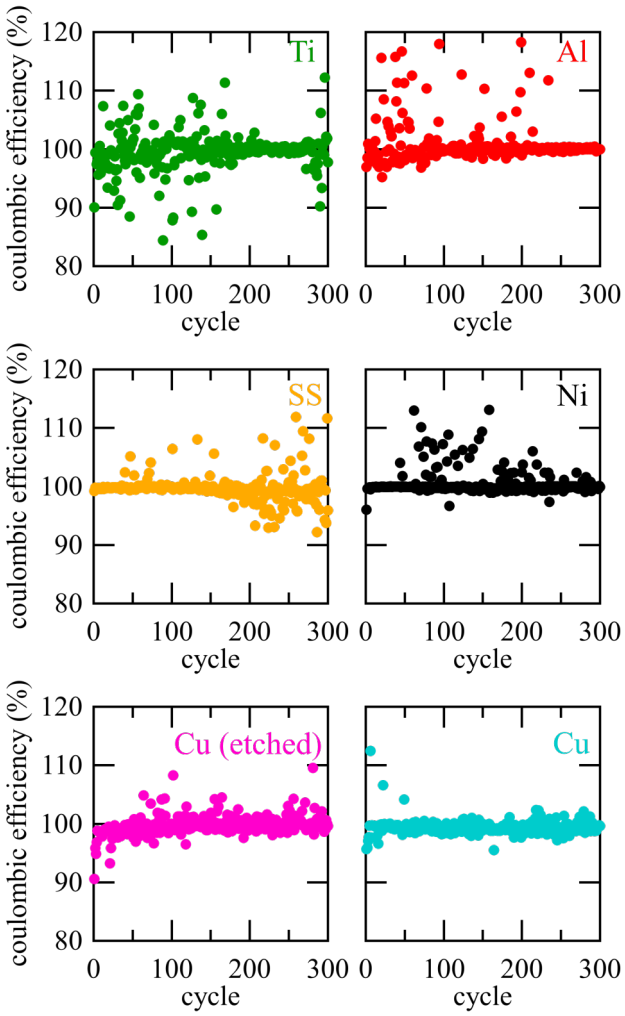

Figure 9: Coulombic efficiencies for the first 300 cycles using different metallic substrates as working electrodes. The half-cells were cycled with the optimal conditions identified: 2 mA/cm² with 30 µl $NaCF_3SO_3$:G2, CG separator, and a HDPE gasket.

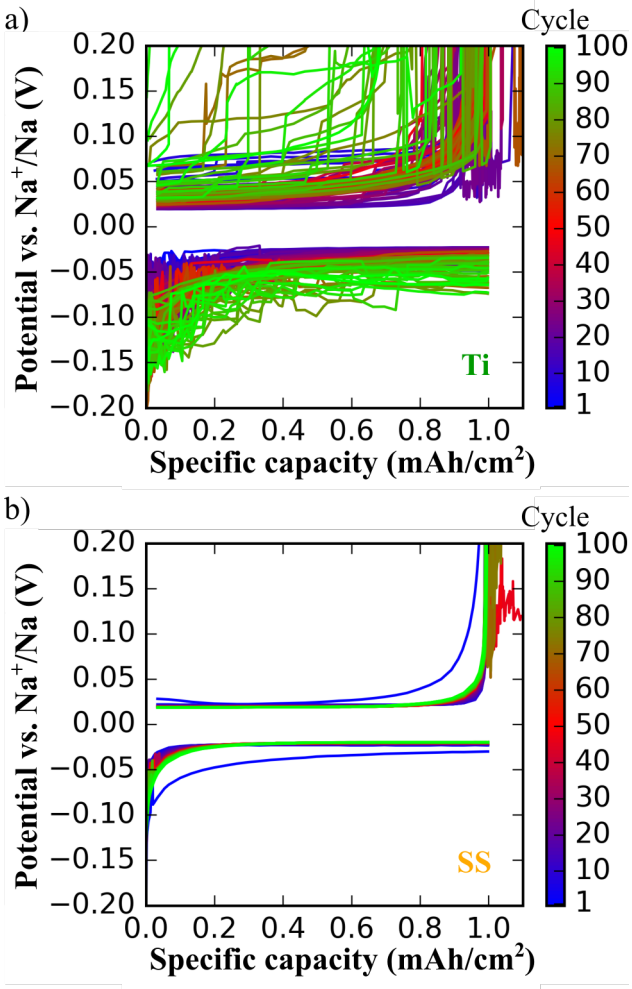

Figure 10: Cycling profiles for (a) titanium and (b) stainless steel substrates. The half-cells were cycled at 2 mA/cm² with 30 µl $NaCF_3SO_3$:G2 soaked in CG.

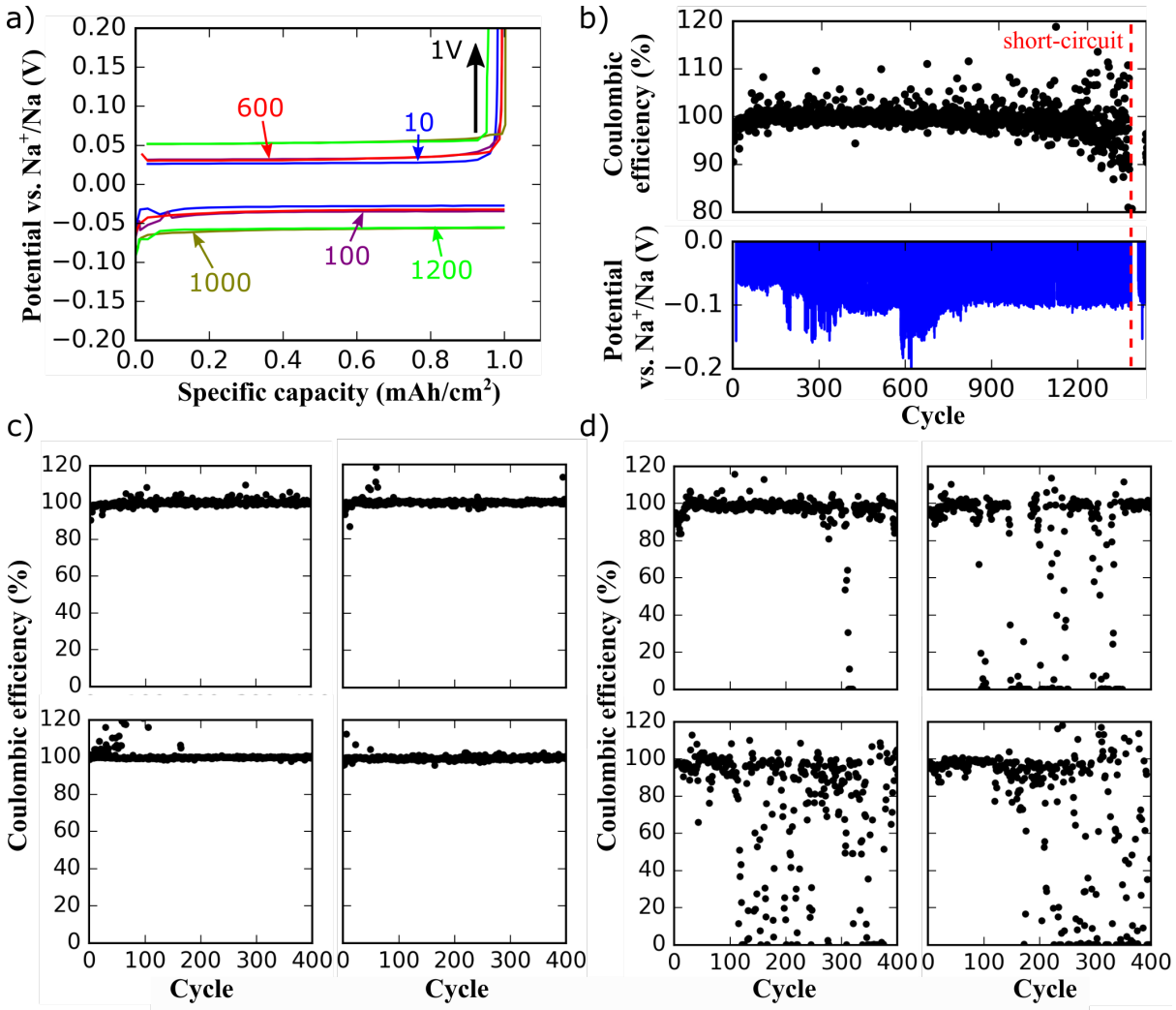

Figure 11: a) Cycling profiles for 30 µl $NaCF_3SO_3$:G2, CG separator, cycled at 2 mA/cm^2, with HDPE gasket on copper. b) CE during long-term cycling of the same cell and its potential during plating. The nucleation potential is being displayed, not the plateau value. The point of failure due to short-circuiting is marked by the red line. Coulombic efficiencies are shown for the first 400 cycles of several cells that were assembled in similar conditions in a glove box with respectively < 0.1 ppm (c) and 1-2 ppm (d) O_2 and H_2O content.